Optical spectra and their moments for sodium clusters, Na_n^+, with $3 \leq n \leq 64$

M. Schmidt and H. Haberland[a]

Fakultät für Physik, Universität Freiburg, H. Herderstr. 3, D-79104 Freiburg, Germany

Abstract. Photoabsorption cross-sections for all sodium cluster ions, Na_n^+, with $n \leq 64$, have been measured at a temperature of about 105 K. The size dependence of the peak positions and widths is discussed. Triaxial deformations are unequivocally observed. The moments of the optical response are calculated from the data and their size dependence discussed. The width of the plasmon peak is not understood.

1 Introduction

Experimental [1–7] and theoretical [8–20] studies of alkali clusters have made them the best understood ones today. This was made possible by a very good interaction between theory and experiment, and the present investigation was started to further deepen this interaction. The optical response of mass selected sodium cluster ions was measured with better signal to noise compared to earlier investigations. This was made possible by an experimental arrangement that allowed to measure the optical response of many clusters at the same time. Moments of the optical response are calculated from which additional useful information can be obtained. The main conclusion of this paper is that the maxima of the absorption peaks and some moments are well understood, while a detailed understanding of the width of the spectral lines is still lacking.

The jellium model has been immensely popular for the calculation of optical spectra [8–11,15–20]. Within this model the valence electrons are treated as completely free, only caged by a constant positively charged background. On the other side, quantum chemical calculations which take into account the positions of the ions are expensive in theoretical input and computing time, but lead to the best results for very small, cold clusters [12–14]. The beginning of an overlap of the two theories has been achieved by including pseudopotentials to the jellium calculation [15–18]. Also the close analogies to nuclear physics have been very inspiring [11,19,20].

[a] e-mail: `hellmut@frha06.physik.uni-freiburg.de`

2 Experiment

The aim of this experiment was to measure photoabsorption cross-sections at one constant temperature as a function of two parameters: 1) the photon energy, and 2) the cluster size. Several measures have been taken, in order to shorten the time for the data taking. A scheme has been published earlier [21], which allowed to shorten this time by a factor of forty or so. Another considerable improvement has been described very recently [22]. The method, which is briefly sketched below, leads to an additional improvement of about a factor of 25, so that both improvements taken together give a reduction of the measuring time by about three orders of magnitude [23].

In all earlier experiments of this group, laser and cluster beam were perpendicular, so that the photons from a pulsed dye laser interacted with only one cluster size at a time. By aligning laser and cluster beam collinearly, as shown in Figure 1, the laser beam interacts with many clusters at the same time. All clusters which are in the first field-free drift space of the time-of-flight mass spectrometer can be measured simultaneously. The collinear arrangement has a second advantage: the overlap between laser and cluster beam is 100%, which makes it much easier to extract the photoabsorption cross-section from the data, as explained in reference [21,24].

The intensity is measured with (I) and without (I_0) laser interaction. For a complete overlap one has

$$I/I_0 = \exp(-\sigma\phi\tau), \tag{1}$$

where ϕ and τ are the laser fluence and pulse length, respectively, and σ is the photofragmentation cross-section. The product $\phi\tau$ can be measured absolutely by a pyroelectric detector (P in Fig. 1). There is a specific difficulty in applying this photofragmentation spectroscopy to larger
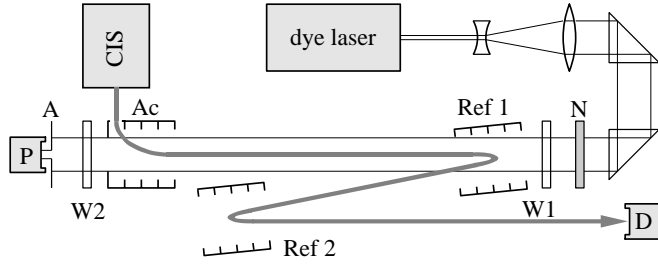
Fig. 1. Schematic diagram of the experiment. Clusters of a temperature of about 105 K are produced in a cluster ion source (CIS). The clusters are deflected by a pulsed accelerator (Ac) and by two reflectrons (Ref 1 and Ref 2) onto the detector D. The beam from the dye laser is enlarged and overlapped collinearly with the cluster beam. One laser pulse interacts with many different cluster sizes, which leads to a large reduction of the measuring time. W1 and W2 = windows for the laser beam, N = neutral density filter, A = diaphragm, and P = pyroelectric photon detector.
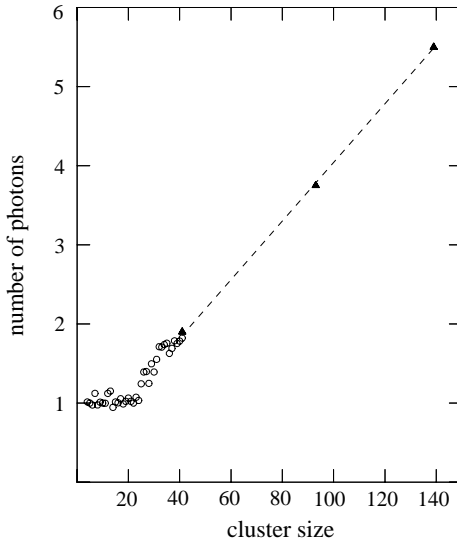

Fig. 2. Number of photons of $\hbar\omega = 2.8$ eV necessary to start the fragmentation of Na_n^+ thermalized at 105 K. The open circles are obtained from a fit of equation (2) to the data. The triangles are from an experiment, where the temperature dependence of the photofragmentation spectra was used to determine thermodynamic properties of clusters [28,29]. One photon is enough to start fragmentation for cluster sizes up to twenty atoms, above $n = 40$ more than two are necessary.

clusters. If the cluster is cold, the absorption of one photon might not heat it enough to induce fragmentation. Whether this effect plays a role is easy to check experimentally. If one photon is enough the intensity I falls exponentially with laser intensity. If two photons are needed $\log[I(\phi\tau)]$ becomes parabolic for small $\phi\tau$.

More specifically, the electronic excitation induced by the photon relaxes fast into vibrations and leads to a heating of the cluster from a temperature of $T_0 \approx 105$ K, to $T_0 + \delta T$, where $k_B \delta T \approx \hbar\omega/(3n - 6)$. For $\hbar\omega = 2.8$ eV and a cluster composed of $n = 25$ atoms one has $\delta T \approx 470$ K, which is not sufficient to fragment the cluster on the time

scale (about 10 μs) of the experiment. The absorption of two photons increases the temperature by about $2\delta T$, which is sufficient for clusters with $n \leq 40$ to fragment, as shown in Figure 2. One can solve the corresponding rate equations, and using the assumption that $\sigma(T_0) = \sigma(T_0 + \delta T)$, one obtains [25,26]:

$$I/I_0 = (1 - \eta) \exp(-\sigma\phi\tau) + \eta(1 + \sigma\phi\tau) \exp(-\sigma\phi\tau), \tag{2}$$

where η is the fraction of clusters needing two photons for fragmentation. From the temperature dependence of the optical absorption one can deduce that the assumption $\sigma(T_0) \approx \sigma(T_0 + \delta T)$ is valid for $n \geq 20$ [22]. Equation (2) can be generalized to the absorption of many photons, but the number of free parameters becomes too large. For very large clusters it is probably advantageous to use the method developed by the Orsay group [27].

Figure 2 shows the mean number of photons of $\hbar\omega = 2.8$ eV which a cluster of 105 K needs to absorb, before it starts to evaporate atoms on a time scale of a few microseconds. This is the interval between the laser pulse and the time the cluster enters the first reflector (Ref 1 in Fig. 1). It is obvious that beginning with about cluster size forty, even two photons are not always enough to induce evaporations. As a result the measured cross-sections are somewhat too small for $n \geq 40$. Nevertheless, also the cluster sizes up $n = 64$ were measured, as it presented hardly any additional work with the present set-up. The data points for $n = 41$, 93, and 139 in Figure 2 have been obtained using the calorimetric techniques developed to study cluster melting [28,29].

A gas aggregation cluster ion source with internal electric discharge was used in this experiment. It was employed without the thermalization stage, thus as shown in Figure 3.14 of reference [30]. A carefully shielded thermocouple measures a temperature of 105 K near the exit of the source, which was taken as the temperature of the clusters.

3 Photoabsorption cross-sections

Figures 3 to 6 show photoabsorption cross-sections in the size range of 3 to 64 atoms per cluster. A small part of the data has been measured earlier [25,31], both sets of data being in perfect agreement. The data agree also with earlier measurements of the Orsay group [32] (only the small dip observed in the spectrum for Na_{21}^+ was not seen here) and with the data of the Copenhagen group [3]. The main difference to these earlier experiments is that 1) the signal-to-noise ratio is much higher here (due to the improvements discussed above) and 2) clusters of a known temperature are studied.

For the small cluster sizes ($n = 3$-9), we observe single, well separated resonances, which could be well fitted by Gaussians. As discussed earlier, the peaks are interpreted as vibrationally broadened electronic transitions of a Na_n^+ *molecule* [12,25,33]. For sodium clusters, vibrational structure could not be resolved. But for Li-clusters
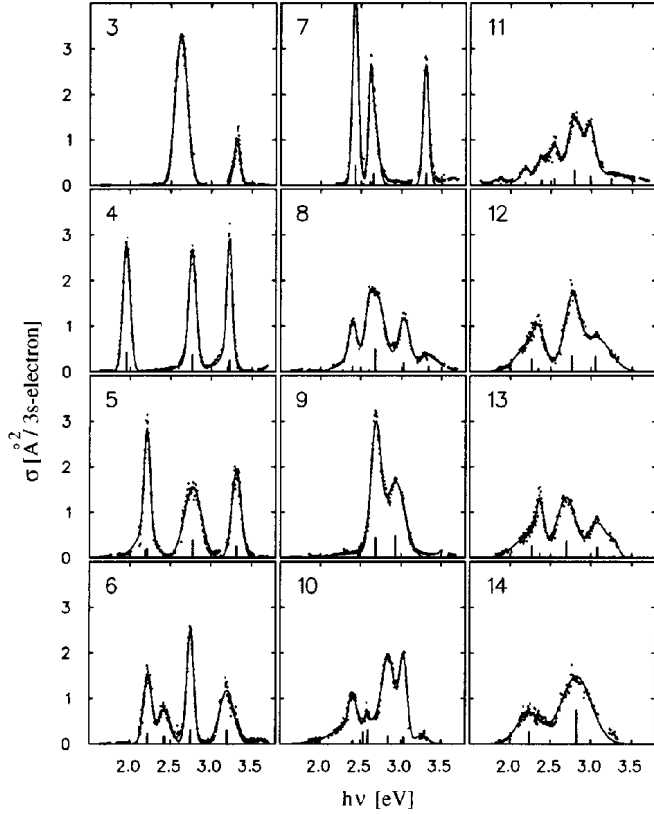
Fig. 3. Photoabsorption cross-section as a function of the photon energy. Plotted is the absolute value per valence electron for cluster sizes between $n = 3$ and 14.

[34,35] we have seen some oscillations which could be interpreted as vibrational structure. The data presented here are in good to fair agreement with Quantum Chemistry type *ab initio* calculations, as discussed elsewhere in detail [12,20,25].

The number of electronic lines increases with cluster size and in the size range $n = 10$ to 15 the lines begin to overlap. For even bigger clusters the single electronic resonances can no longer be resolved. Instead we observe envelopes which can be characterized by one, two, or three Lorentzian peaks, which were fitted by

$$\sigma(E) = \frac{\hbar e^2}{m_e c \epsilon_0} \sum_{i=1}^{3} \frac{f_i E^2 \Gamma_i}{(E^2 - E_i^2)^2 + (E\Gamma_i)^2}, \quad (3)$$

where m_e is the bare electronic mass, and $E = \hbar\omega$ the photon energy. The oscillator strength f_i, the peak positions E_i and the width of the single resonances Γ_i were used as fit parameters with the restriction that the oscillator strength of all the resonances is identical ($f_1 = f_2 = f_3$). When two resonances were sufficient to describe the spectrum, $f_1 = 2f_2$ was demanded. Fit curves are included in Figures 3 to 6. The numerical values are given in Table 1. The peak positions are given by the vertical sticks in Figures 3 to 6 and in Figure 8a.

The larger the cluster size, the stronger is an additional broad absorption on the high-energy side of the optical spectrum. This can have two origins: 1) it could be
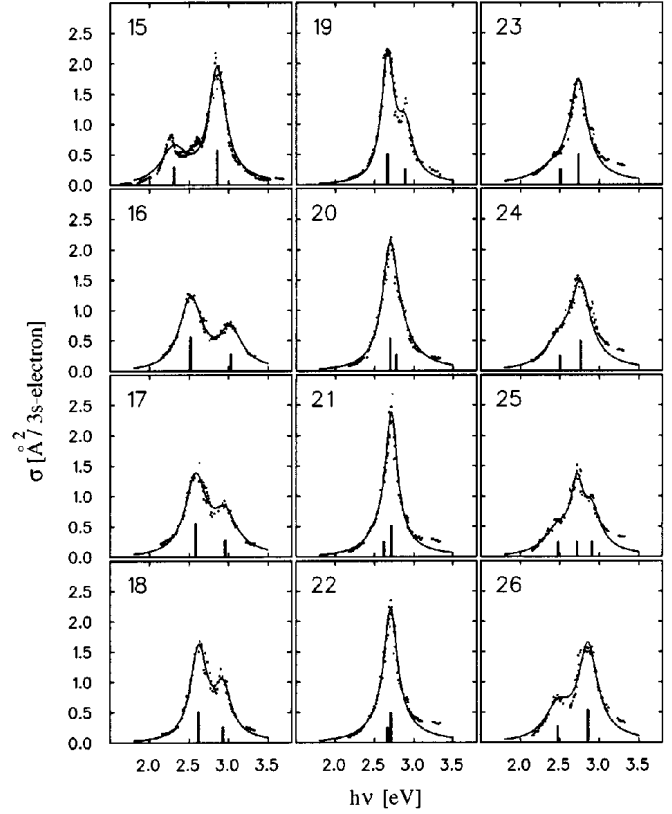

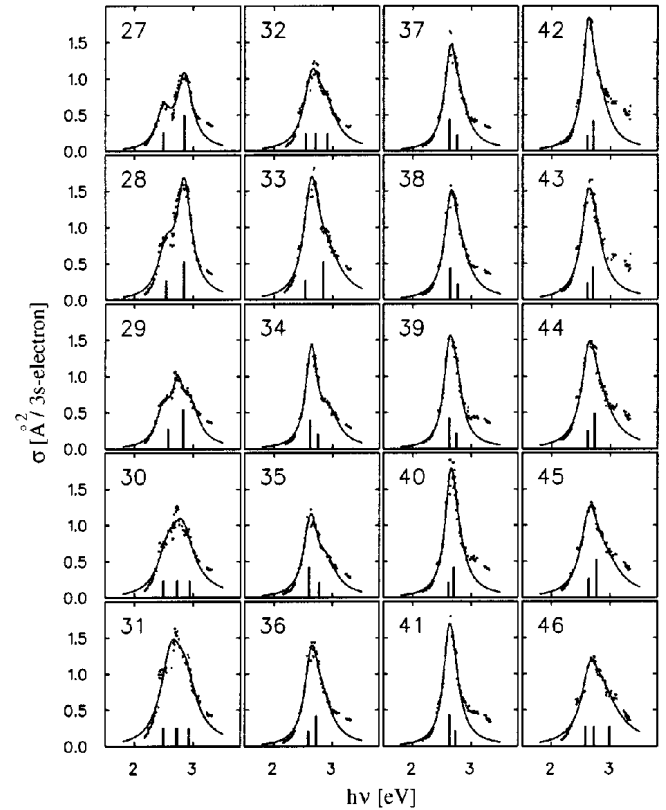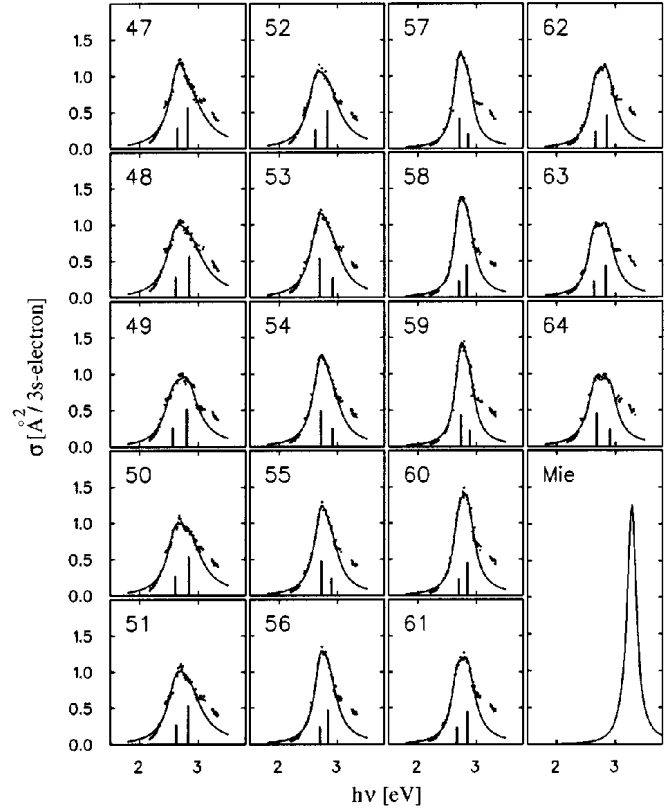**Fig. 4.** As in Figure 3 but for $n = 15$ to 26.

Fig. 5. As in Figure 3 but for $n = 27$ to 46.

Table 1. Fitting parameters for the optical data, as given by equation (3).

n	E_1	Γ_1	E_2	Γ_2	E_3	Γ_3
9	2.697	0.150	2.963	0.137	-	-
10	2.916	0.328	2.406	0.396	-	-
11	2.860	0.371	2.459	0.514	-	-
12	2.786	0.252	2.299	0.208	-	-
13	2.707	0.180	2.345	0.206	3.110	0.283
14	2.827	0.357	2.236	0.432	-	-
15	2.852	0.258	2.307	0.417	-	-
16	2.518	0.348	3.023	0.335	-	-
17	2.581	0.330	2.956	0.353	-	-
18	2.621	0.263	2.926	0.251	-	-
19	2.665	0.194	2.889	0.242		
20	2.695	0.238	2.776	0.444	-	-
21	2.715	0.181	2.617	0.467	-	-
22	2.705	0.203	2.665	0.576	-	-
23	2.736	0.253	2.507	0.709	-	-
24	2.760	0.301	2.502	0.457	-	-
25	2.906	0.278	2.480	0.424	2.716	0.186
25	2.908	0.282	2.481	0.428	2.717	0.187
26	2.856	0.291	2.477	0.400	-	-
27	2.845	0.312	2.486	0.307	-	-
28	2.840	0.296	2.533	0.354	-	-
29	2.733	0.239	2.495	0.321	2.957	0.335
29	2.820	0.506	2.568	0.422	-	-
30	2.935	0.280	2.489	0.286	2.723	0.204
30	2.763	0.318	2.496	0.310	-	-
31	2.792	0.420	2.537	0.347	-	-
31	2.919	0.284	2.485	0.262	2.714	0.202
32	2.737	0.315	2.559	0.284	-	-
32	2.706	0.192	2.539	0.263	2.909	0.272
33	2.702	0.273	2.546	0.252	-	-
34	2.616	0.206	2.753	0.248	-	-
35	2.599	0.242	2.769	0.232	-	-
36	2.724	0.276	2.587	0.191	-	-
37	2.630	0.243	2.760	0.249	-	-
38	2.636	0.259	2.768	0.261	-	-
39	2.620	0.236	2.745	0.223	-	-
40	2.704	0.263	2.611	0.197	-	-
41	2.626	0.239	2.726	0.357	-	-
42	2.702	0.348	2.603	0.192	-	-
43	2.697	0.407	2.607	0.259	-	-
44	2.730	0.450	2.610	0.270	-	-
45	2.765	0.581	2.632	0.297	-	-
46	2.852	0.674	2.649	0.329	-	-
46	2.718	0.291	2.577	0.404	2.983	0.423
47	2.685	0.207	2.518	0.351	2.889	0.284
47	2.814	0.634	2.640	0.312	-	-
48	2.836	0.612	2.605	0.364	-	-
48	2.924	0.305	2.507	0.337	2.700	0.248
49	2.805	0.460	2.562	0.360	-	-
49	2.694	0.222	2.490	0.295	2.882	0.234
50	2.711	0.303	2.554	0.357	2.938	0.361
50	2.832	0.537	2.601	0.330	-	-
51	2.820	0.549	2.616	0.344	-	-
52	2.821	0.513	2.622	0.322	-	-
53	2.695	0.387	2.915	0.439	-	-
54	2.712	0.328	2.912	0.389	-	-
55	2.721	0.313	2.894	0.358	-	-
56	2.835	0.369	2.697	0.230	-	-
57	2.711	0.250	2.862	0.232	-	-
58	2.835	0.310	2.702	0.196	-	-
59	2.737	0.243	2.885	0.242	-	-
60	2.845	0.299	2.701	0.229	-	-
61	2.844	0.329	2.672	0.240	-	-
62	2.850	0.356	2.658	0.258	-	-
63	2.830	0.354	2.629	0.245	-	-
64	2.679	0.366	2.906	0.281	-	-

Fig. 6. As in Figure 3 but for $n = 47$ to 64. The last spectrum, marked "Mie", has been calculated as discussed in the context of equation (6).

the beginning of the volume plasmon modes [7–9], or 2) it could be the microscopic analogue of the bulk interband transition (see Section 6.1 below). The data on the high-energy side cannot be described by a Lorentzian or Gaussian peak shape and thus were neglected for the fit to equation (3).

4 Discussion of the optical spectrum

4.1 Peak positions

In the jellium model, one has a closed electronic shell for $n = 8, 20, 40, 58 \ldots$ valence electrons. This gives a spherical shape for the cluster, and one dominant line in the spectrum. Very deformed, asymmetric structures have been calculated for open shell clusters [36,37]. For the interpretation of the optical spectra of the larger clusters it has been sufficient so far to treat the cluster as a spheroid. The data suggest that often two axes are identical (or differ not too much from another). This gives either a prolate (cigar-like) or oblate (disc-like) deformation. If two of the principle axes are identical, the resonances along them are degenerate in energy and the optical peak thus of about double intensity. As the resonance parallel to the longer axis has a lower frequency, one can deduce the cluster's shape from a simple inspection of the optical spectrum.
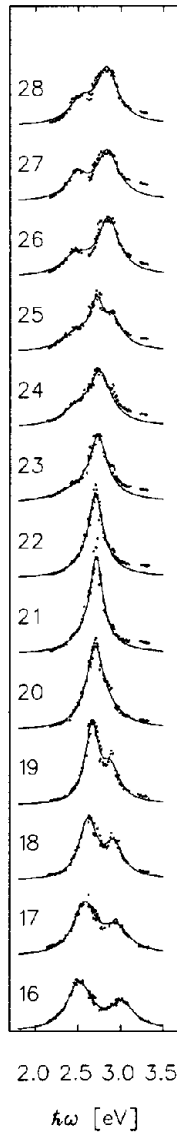
Fig. 7. Cluster sizes between 16 and 20 are oblate, above $n = 23$ they are prolate. The spherical shape of the Na_{21}^+ cluster leads to the narrowest line.
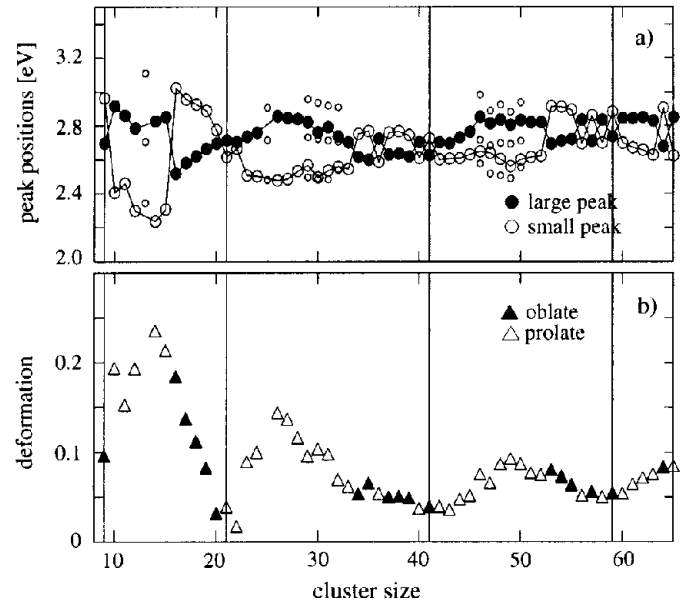

Fig. 8. Peak energies as a function of cluster size are shown in the upper figure (a). The energies have been obtained by a Lorentz-fit to the data (see Eq. (3)). The position of the intense peak is given by a full circle, the position of the less intense peak by a large open circle. Three small open circles are shown where a three peak fit is possible. Closed electronic shells are indicated by the vertical lines. The lower figure (b) shows the deformation parameter Δ of equation (4), plotted against the cluster size. Full triangles indicate oblate, open circles prolate deformations.

An example is shown in Figure 7. For the spherical symmetric Na_{21}^+ one has one single peak, and a change-over from an oblate at smaller to a prolate geometry at larger cluster sizes.

The location of the peak maxima up to $n = 66$ are given in Figure 8a. If the more intense peak (marked by a full dot) has a higher energy, one has a prolate structure, and *vice versa*. There is a change from oblate to prolate geometry at each closed shell, and also one in between closed shells. For some clusters one could also make a fit with three peaks of equal intensity, corresponding to a triaxial structure. These are indicated by three small open dots in Figure 8a. Triaxial shapes have been calculated for neutral sodium clusters using the jellium approximation in references [9,38–40]. These authors calculated the ground state and find triaxial deformations for $N = 11$–13, 23–25,

61–65 ... valence electrons. In the optical spectrum, we find an indication of a possible triaxial shape for $N = 12$, 24, 28–31, 44–48 valence electrons.

The Nillson-Clemenger model [41] predicts that the inverse ratio of the two axes R_1 and R_2 of a deformed cluster equals the ratio of the resonance energies. The connection between the energetic splitting of the resonances and the deformation is given by

$$\Delta = \frac{\Delta R}{\bar{R}} = 2\frac{|R_1 - R_2|}{R_1 + R_2} = 2\frac{|E_2 - E_1|}{E_1 + E_2} . \qquad (4)$$

The result is shown in Figure 8b. The deformation Δ is smallest—but not zero—for spherical clusters. Many authors have derived results similar to equation (4) as discussed in detail in reference [3].

4.2 Width of a single line

Contrary to the peak positions, the width of the spectrum is not well understood so far. The only general agreement seems to be that the total width of a spectrum cannot be due to a lifetime effect. This is very evident from the discussion above and an inspection of Figure 8b, which shows that the geometric deformations of a single cluster has a large contribution to the overall linewidth.

It has been discussed above, that save for the peak at the high-energy side, the experimental peaks are well
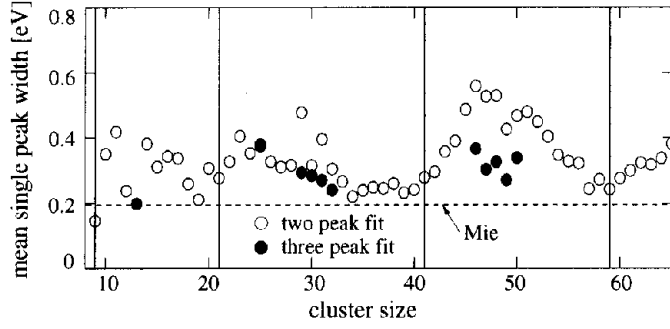
Fig. 9. Mean single peak widths as a function of cluster size. Note, that all spherical clusters and the Mie plasmon have a line width of about 0.2 eV.

represented by Lorentzians. Figure 9 shows the Γ values as defined by equation (3), *i.e.* the width of each single line in the spectrum is plotted. The result is surprising. There is no systematic shift with cluster size, if one disregards the shell effects. Also the value for the Mie plasmon lies in the same range. As the Γ values are obtained from a Lorentz fit, one is tempted to interpret the width as being due to a lifetime τ:

$$\Gamma = \hbar/\tau\,. \tag{5}$$

With $\hbar = 0.656$ fs·eV one obtains lifetimes of the order of 1.5 to 3.5 fs for a linewidth of 0.2 to 0.4 eV. This value seems to be too short, as discussed in more detail below.

4.3 Asymptotic limit

The classical equation for light absorption by a small sphere of radius R reads [42,43]:

$$\sigma(\hbar\omega) = \frac{4\pi\omega}{c}R^3\mathrm{Im}\left(\frac{\epsilon(\omega)-1}{\epsilon(\omega)+2}\right)\,. \tag{6}$$

Here Im stands for the imaginary part, and $\epsilon(\omega)$ is the complex dielectric function. Using the experimental $\epsilon(\omega)$ for sodium [44], one obtains the absorption profile given as the last curve in Figure 6 (marked Mie). The curve has a maximum at $E_{\mathrm{Mie}} = 3.27$ eV; note that this is different from the pure jellium result of 3.41 eV. The small but significant difference of 140 meV is attributed to core polarization effects, *i.e.* the interaction of the 3s-electrons with the much stronger bound core electrons [45]. This effect is not incorporated in the jellium model, but could be taken care of by an effective electron mass. The full width at half maximum is 0.173 eV which corresponds to a variance of $\delta = 0.196$ (for a definition of δ see Eq. (12)). The oscillator strength between 1.5 and 3.7 eV is $f = 0.77$ per electron. These asymptotic values are included in Figures 10 and 11.

5 Sum rules and moments

Independent of the specific form of the optical response, there is additional valuable information in the integrals of
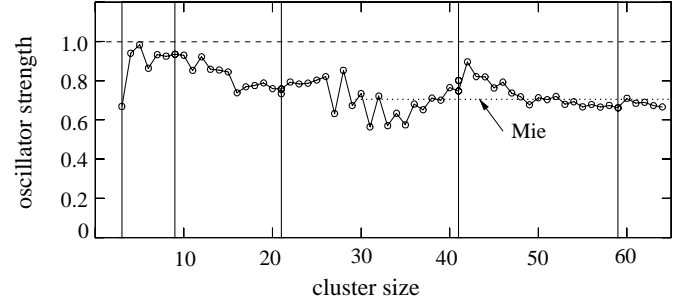

Fig. 10. Oscillator strength between 1.5 and 3.7 eV as a function of cluster size, calculated by equation (8). A value of only 0.77 is obtained for the Mie plasmon in this limited energy range, due to the cut-off imposed by the upper limit of the photon energy used. Note, that starting with Na_{26}^+ up to at least Na_{60}^+ all odd cluster sizes show a significantly higher oscillator strength in the measured range than the even ones. The estimated error for the smaller clusters is below 10%, resulting mainly from the fact that laser beam profile is not completely flat.

the spectra [9]. The moment M_k is defined as [46]

$$M_0 = \int_0^\infty \sigma(E)\mathrm{d}E \quad \text{for} \quad k = 0\,,$$

$$M_k = \int_0^\infty E^k\sigma(E)\mathrm{d}E/M_0 \quad \text{for} \quad k > 0\,. \tag{7}$$

Experimental information for several moments will be discussed now.

5.1 Oscillator strength

For $k = 0$ one obtains the Thomas-Reiche-Kuhn sum rule for the oscillator strength f, which states that the zeroth moment is proportional to the number $N(e^-)$ of electrons.

$$f = \frac{2m_{\mathrm{e}}c\epsilon_0}{\pi\hbar e^2}M_0 = \frac{0.911}{\mathring{A}^2 eV}\int\sigma\mathrm{d}E = N(e^-)\,. \tag{8}$$

This is an exact equation giving $f(\text{total}) = 11$ if the integral is extended over all photon energies. In the experiment we have measured $\sigma(E)$ only between 1.5 and 3.7 eV, so the integral can only be extended over this finite energy interval, where the absorption of the 3s-electrons occurs. In all the integrals of this section these finite limits are implied.

Under certain conditions one can decompose the sum rule and obtain the oscillator strength due to just one electron. For sodium, with its $1s^22s^22p^63s$ electronic structure, one writes:

$$f(\text{total}) = f(1s, 2s, 2p) + f(3s)\,. \tag{9}$$

The approximation $f(3s) = 1$ (per atom) is very good for sodium as: i) the optical spectrum due to the 3s-electrons is well separated from that of the other electrons, and ii) the interaction of the 3s electrons with the other electrons can be well approximated by a local pseudopotential [47].
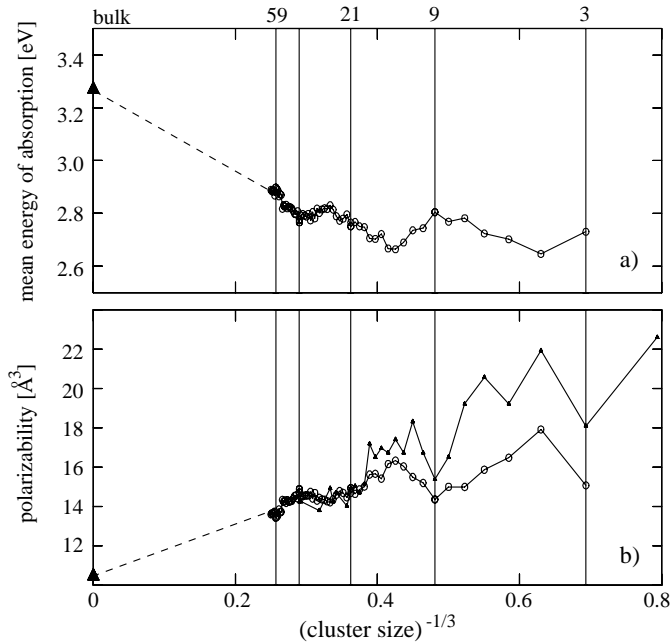
Fig. 11. (a) Mean peak energies of the optical spectra (Eq. (10)). Closed electronic shells are indicated by vertical lines. (b) Polarizability per $3s$ electron of neutral (from Ref. [48]) and charged clusters (Eq. (11)). The plot for neutral clusters has been shifted by one mass, so that clusters with the same number of valence electrons are vertically above one another.

From the many jellium calculations one gets exactly $f = 1$ per $3s$ electron for sodium. Integrating the experimental spectra one obtains, for $n \geq 15$, that more than 85% of the maximal oscillator strength contributes to the experimental data. The results are given in Figures 10. We expect that the remaining 15% are hidden in the energy range above 3.7 eV, the highest energy used in this experiment. It can be seen from Figure 3 to 6 that the cross-section is not zero at the highest photon energies used experimentally. This is in agreement with the fact, that the oscillator strength for the limiting Mie plasmon is also only $f(R \to \infty) = 0.77$ per valence electron if one takes into account the limited photon range of this experiment.

This discussion does not apply to the very small sizes. For $n = 2$ and 3 the photon reaches states which to not dissociate in the time scale of the experiment; *i.e.* the dimer and trimer have only a probability of about 1/3 or 2/3 to dissociate, respectively. This can be understood in term of symmetry arguments as discussed elsewhere [25].

5.2 Mean transition energy

The first moment, M_1, is proportional to the mean transition energy:

$$\langle \hbar \omega \rangle = M_1 . \tag{10}$$

Experimental values of are shown in Figure 11a. As could be expected, the stronger bound electrons in the closed
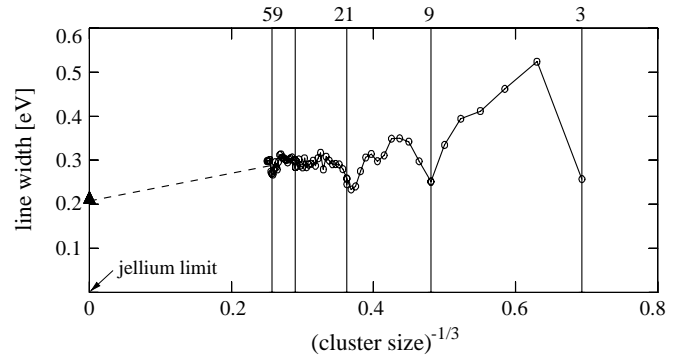

Fig. 12. Mean square deviation δ of the optical spectra as defined by equation (12).

shell clusters have a higher mean resonance energy compared to the electrons in open shell clusters of similar size. It has been shown in reference [22] hat this mean transition energy is nearly independent of temperature.

5.3 Polarizability

The polarizability α is proportional to the minus second moment:

$$\alpha = \frac{e^2 \hbar^2}{m} M_{-2} . \tag{11}$$

Experimental results are shown in Figure 11b. They also show some structure due to electronic shell closings. Included in Figure 11b are directly measured polarizabilities of the Knight group for neutral sodium clusters [48]. For $N(e^-) \geq 17$ the two polarizabilities agree. Only for smaller clusters, is the α(neutral cluster) higher than that for charged ones. This is physically plausible. The extra charge leads to a stronger bond of the electrons, which are thus less polarizable by an external electric field. The smaller the cluster becomes, the more pronounced this effect becomes. For the extrapolation to $R \to \infty$ one again expects a smooth R^{-1} dependence.

It has been discussed above that clusters with more than 40 atoms need more than two photons to fragment. This leads to a nearly negligible systematic error for the moments. For Na_{64}^+ the mean excitation energy is slightly too big, and the polarizability slightly to small; all errors being smaller then 3%.

5.4 Total width of the spectrum

The variance δ around M_1

$$\delta^2 = \int (E - M_1)^2 \sigma(E) \mathrm{d}E / M_0$$
$$= M_2 - M_1^2 , \tag{12}$$

is a measure of the width of the spectrum. Figure 12 shows the results. One observes large variations. For all closed

electronic shells, save $N(e^-) = 40$, the spectral width has a minimum. The value of δ is a measure of the total width of the spectrum; it is dominantly given by the deformation effects of the open shell clusters as given by equation (4). It should be distinguished from the single line peak width as defined by equation (3) and given in Figure 9 which is discussed now.

6 Discussion of the width of the spectra

The width of a *single* line of the spectra has several origins. The main contributions are: 1) fragmentation of the spectral width, which can only be calculated, 2) broadening due thermal effects (see Ref. [22]), and 3) lifetime effects as given by equation (5). How these different contributions interact to give the total lineshape observed experimentally has so far never been studied theoretically.

6.1 Width of the bulk Mie plasmon

The dipolar response of a large sodium sphere can be calculated from the experimental bulk dielectric function as discussed in the context of equation (6). The calculated width is $\Gamma_0 = 0.19$ eV. This asymptotic "experimental" width is due to a structure in the dielectric function which is caused by an interband transition [49]. The collective oscillation can decay by exciting a single electron to a higher electronic band. The same mechanism occurs in the damping of the bulk plasmon, where the width can be well correlated with the strength of the pseudopotential (see Fig. 9 of Ref. [45]). If the width Γ_0 were entirely due to a lifetime effect, this would correspond according to equation (5), to $\tau \approx 3.5$ fs.

The word "interband" is defined only for a crystalline lattice. The question thus arises how this concept can be generalized to a finite system. This is relatively simple for the alkalis: In the bulk, the k-value of the interband transition is not so far from the edge of the Brillouin zone [49]. At the very edge of the Brillouin zone, an interband transition can be discussed in real space, namely that electronic charge is taken from the position of the nuclei to positions between the nuclei [49,50]. This concept can easily be applied to a finite system. Evidently, in a jellium type calculation this cannot occur. There are no atoms from which the electrons could scatter and thus no band structure. It is therefore plausible that all these calculations [9,11,33, 51–53] yield $\Gamma_0 = 0$. A calculation using pseudopotentials should be able to capture this point.

6.2 Scaling laws

The size dependence of the widths has been studied by several theoretical groups [9,11,33,51–53]. The jellium model was used nearly exclusively. In this case, the interband decay of the plasmon discussed above is not possible, and the collective plasmon oscillations can only decay by exciting a single electron from the same band, a process which has been termed Landau damping. For sufficiently large clusters this gives a width like (Eq. 9.7 of Ref. [11]):

$$\Gamma = C_1 v_{\text{Fermi}}/R, \qquad (13)$$

where v_{Fermi} is the Fermi velocity ($1.07 \cdot 10^6$ m/s for bulk sodium), R the cluster radius and C_1 a constant varying for spherical clusters between 0.55 [31,54] and 0.75 [52]. In the dipolar bulk limit one obtains a vanishing width from equation (13), *i.e.* $\Gamma(R \to \infty) = 0$. From the bulk dielectric function, on the other hand one calculates a width of $\Gamma_0 = 0.19$ eV. A better representation of the experimental data might therefore be

$$\Gamma = \Gamma_0 + C_1 v_{\text{Fermi}}/R. \qquad (14)$$

This equation has the expected size dependence and the correct limit for arbitrarily large clusters. Our data point to a value which is a factor of 3 to 5 smaller than given by equation (14). We conclude from this discrepancy, that if there is some applicability of equations (13) and (14) to real clusters it becomes applicable only for larger ones than studied here. Note, that if equations (13) and (14) are valid, the width Γ has a maximum as a function of cluster size. This has indeed been observed theoretically [53,55].

In the jellium model, clusters with a closed electronic shell are perfect spheres. Experimentally, one cannot avoid some surface roughness, which can have two origins: thermal or geometric. Thermal line broadening has been discussed elsewhere [22]. The thermally induced surface roughness was recently calculated [56]. At 100 K one obtains a rms roughness of about $\Delta \approx 0.4$ Å. Converting this to thermally induced width gives a value which is a little high, but not too much. In the same spirit, one would expect also a contribution from geometric disorder, *i.e.* from atoms outside closed geometric shells. An alternative treatment is given by the random matrix model [57], good agreement has been obtained for the width of Na_{21}^+.

In principle, one would expect that all the broadening effects add up leading to rather broad lines which is not observed experimentally. One has to conclude that a detailed understanding of the line shapes of the plasmon peaks is still missing.

6.3 Lifetime of the resonance

The linewidths of Figure 9 are 0.2 to 0.4 eV. According to equation (5) this gives a lower limit for the lifetime of 1.6 to 3.3 fs. One obtains only a lower limit, as non-lifetime related broadening effects have not been corrected for. There exists only one measurement of the lifetime for a free sodium cluster ion which gives for the lifetime of the collective resonance of Na_{93}^+ a value of $\delta t = 10$ to 20 fs [58]. This would correspond to a lifetime broadening of only $\Gamma = 33$ to 66 meV. As this is much smaller than the total width one can conclude: 1) The lifetime contribution to the plasmon linewidth is small (at least for Na_{93}^+), and 2) the near Lorentzian shape of the single lines is not due to a lifetime effect.

There exist two studies of the plasmon lifetime of large sodium clusters on a dielectric surface. One study obtains a value of 10 to 15 fs, after correcting for the inhomogeneous broadening due to the experimentally unavoidable cluster size distribution [59]. The other experiment obtains a cluster-size-dependent lifetime of 2 to 10 fs, without performing this correction [60].

7 Summary

The size dependence of the optical response has been measured for positively charged sodium cluster ions, Na_n^+, $4 \leq n \leq 64$. A transition from single, molecular, Gaussian-shaped resonances to collective, Lorentzian-shaped peaks has been observed. Deformation of the open shell cluster leads to a splitting into two or three peaks as predicted by theory. The mean absorption energy and the polarizability, which have been calculated by a moment analysis of the spectra, show electronic shell closings as well as the right tendency in the development toward the bulk values. No general size dependence of the peak width could be observed. The width of the spectral lines as well as the plasmon lifetimes have been discussed. Both are not understood in detail so far.

References

1. W.D. Knight, K. Clemenger, W.A. de Heer, W.A. Saunders, M.Y. Chou, M.L. Cohen, Phys. Rev. Lett. **52**, 2141 (1984).
2. C. Bréchignac, Ph. Cahuzac, F. Carlier, M. de Frutos, J. Leygnier, Chem. Phys. Lett. **189**, 28 (1992); C. Bréchignac in [30].
3. J. Borggreeen, P. Chowdhury, N. Kebaïli, L. Lundsberg-Nielsen, K. Lützenkirchen, M.B. Nielsen, J. Pedersen, H.D. Rasmussen, Phys. Rev. B **48**, 17507 (1993).
4. C. Wang, S. Pollack, T. Dahlseid, G.M. Koretsky, M.M. Kappes, J. Chem. Phys. **96**, 7931 (1992).
5. T. Baumert, R. Thalweiser, V. Weiß, G. Gerber, Z. Phys. D **26**, 131 (1993).
6. H. Fallgren, K.M. Brown, T.P. Martin, Z. Phys. D **19**, 81 (1991).
7. W.A. deHeer, Rev. Mod. Phys. **65**, 611 (1993).
8. W.E. Ekardt, Phys. Rev. B **31**, 6360 (1985).
9. M. Brack, Rev. Mod. Phys. **65**, 677 (1993).
10. M. Brack, Sci. Am. **12**, 32 (1977).
11. G.F. Bertsch, R.A. Broglia *Oscillations in Finite Quantum Systems* (Cambridge University press, 1994).
12. V. Bonačić-Koutecký, J. Pittner, C. Fuchs, P. Fantucci, M.F. Guest, J. Koutecký, J. Chem. Phys. **104**, 1427 (1996).
13. U. Röthlisberger, W. Andreoni, J. Chem. Phys. **94**, 8129 (1991).
14. V. Bonačić-Koutecký, J. Jellinek, M. Wiechert, P. Fantucci, J. Chem. Phys. **107**, 6321 (1997).
15. F. Alasia, Ll. Serra, R.A. Broglia, N. Van Giai, E. Lipparini, H.E. Roman, Phys. Rev. B **52**, 8488 (1995).
16. S.A. Blundell, C. Guet, Z. Phys. D **33**, 153 (1995).
17. W.D. Schöne, W. Ekardt, J. Pacheco, Phys. Rev. B **50**, 11078 (1997); J.M. Pacheco, W.D. Schöne, Phys. Rev. Lett. **79**, 4989 (1997).
18. J.M. Pacheco, W.D. Schöne, Phys. Rev. Lett. **79**, 4989 (1997).
19. R.A. Broglia, J.M. Pacheco, C. Yannouleas, Phys. Rev. B **44**, 5901 (1991).
20. W. Ekardt (Editor), *Metal Clusters*, J. Wileys Ser. Theor. Chem. (1999).
21. Ch. Ellert, M. Schmidt, Ch. Schmitt, Th. Reiners, H. Haberland, Phys. Rev. Lett. **75**, 1731 (1995).
22. M. Schmidt, Ch. Ellert, W. Kronmüller, H. Haberland, to be published in Phys. Rev. B.
23. M. Schmidt, Ph.D. thesis, Freiburg (1996).
24. H. Haberland, B. v. Issendorff, Phys. Rev. Lett. **76**, 1445 (1996).
25. Ch. Ellert, M. Schmidt, Th. Reiners, H. Haberland, Z. Phys. D **39**, 317 (1997).
26. Ch. Schmitt, Ch. Ellert, M. Schmidt, H. Haberland, Z. Phys. D **42**, 145 (1997).
27. C. Bréchignac, Ph. Cahuzac, J. Leygnier, A. Sarfati, Phys. Rev. Lett. **70**, 2036 (1993).
28. M. Schmidt, R. Kusche, W. Kronmüller, B. v. Issendorff, H. Haberland, Phys. Rev. Lett. **79**, 99 (1997).
29. M. Schmidt, R. Kusche, B. v. Issendorff, H. Haberland, Nature **393**, 238 (1998).
30. H. Haberland (Editor), *Clusters of Atoms and Molecules I*, Spring. Ser. Chem. Phys., Vol. 52 (Springer-Verlag, 1999).
31. Th. Reiners, Ch. Ellert, M. Schmidt, H. Haberland, Phys. Rev. Lett. **74**, 1558 (1995).
32. C. Bréchignac, Ph. Cahuzac, F. Carlier, M. de Frutos, J. Leygnier, Chem. Phys. Lett. **189**, 28 (1992).
33. G. Bertsch, D. Tománek, Chem. Phys. Lett. **205**, 521 (1993).
34. Ch. Ellert, M. Schmidt, M. Kronmüller, H. Haberland, to be published.
35. Ch. Ellert, Ph.D. Freiburg, 1995 (unpublished).
36. M. Koskinen, P.O. Lipas, M. Manninen, Nucl. Phys. A **591**, 421 (1995).
37. S. Frauendorf, V.V. Pashkevich, Ann. Phys. (Leipzig) **5**, 34 (1996).
38. C. Yannouleas, U. Landman, Phys. Rev. B **51**, 1902 (1995).
39. S.M. Reimann, S. Fraundorf, M. Brack, Z. Phys. D **34**, 125 (1995).
40. S. Kasperl, C. Kohl, P.-G. Reinhard, Phys. Lett A **206**, 81 (1995).
41. K. Clemenger, Phys. Rev. B **32**, 1359 (1985).
42. G.F. Bohren, D.R. Huffman *Absorption and Scattering of Light from Small Particles* (Wiley, New York, 1983).
43. W. Ekardt, Z. Penzar, Phys. Rev. B **43**, 1322 (1991).
44. N.V. Smith, Phys. Rev. **183**, 634 (1969).
45. A. vom Felde, J. Sprösser-Prou, J. Fink, Phys. Rev. B **40**, 10181 (1989).
46. A different definition of the moment is often used in theoretical papers. The k-th moment as defined here is proportional to the $(k + 1)$ moment of imaginary part of the dynamical polarizability as defined by equation 4.11 of [9].
47. C. Guet, Comm. At. Mol. Phys. **31**, 305 (1995).

48. W.D. Knight, K. Clemenger, W.A. de Heer, W.A. Saunders, Phys. Rev. B **31**, 2539 (1985).
49. N.W. Ashcroft, N.D. Mermin, *Solid State Physics* (Saunders College, Philadelphia, 1976), see figs. 15.9 and 15.10.
50. We acknowledge an illuminating discussion with M. Cohen/Berkeley on this point.
51. R.A. Broglia, J.M. Pacheco, Phys. Rev. B **62**, 1400 (1989).
52. C. Yannouleas, R.A. Broglia, Ann. Phys. (N.Y.) **217**, 105 (1992).
53. C. Yannouleas, Phys. Rev. B **58**, 6748 (1998).
54. A. Liebsch, Phys. Rev. B **36**, 7378 (1987).
55. J. Babst, P.G. Reinhard, Z. Phys. D **42**, 209 (1997).
56. N. Pavloff, C. Schmitt, Phys. Rev. B **58**, 4942 (1998).
57. V.M. Akulin, C. Bréchignac, A. Sarfati, Phys. Rev. B. **55**, 1372 (1997).
58. R. Schlipper, R. Kusche, B. v. Issendorff, Phys. Rev. Lett. **80**, 1194 (1998).
59. M. Simon, F. Träger, A. Assion, B. Lang, S. Voll, G. Gerber, Chem. Phys. Lett. accepted for publication
60. J.-H. Klein-Wiele, P. Simon, H.-G. Rubahn, Phys. Rev. Lett. **80**, 45 (1998).